Azimuthal modulation of cosmic ray flux as an effect of geomagnetic field in the ARGO-YBJ experiment

R. Assiro [1] , P. Bernardini [1] [2] , A. Corvaglia [1], P. Creti [1], A. D'Amone [1] [2], I. De Mitri [1] [2], G. Mancarella [1] [2], G. Marsella [1] [3] , D. Martello [1] [2], M. Panareo [1] [3], L. Perrone [1] [3], C. Pinto [1] [2], S. Sbano [1] [2], A. Surdo [1]

[1] Istituto Nazionale di Fisica Nucleare, sez. di Lecce, Italy

[2] Dipartimento di Fisica, Università del Salento, Italy

[3] Dipartimento di Ingegneria dell'Innovazione, Università del Salento, Italy

Cosmic rays (CRs) are charged particles and their paths are deflected by the magnetic fields. The galactic magnetic field randomizes the CR arrival directions. The geomagnetic field restrains low-rigidity CRs from reaching the terrestrial atmosphere and causes that the CR flux is lower from East than from West. The geomagnetic field acts also on the charged particles of the extensive air showers (EAS) during their path of few kilometers in the atmosphere. Cocconi [1] suggested that the lateral displacement induced by the Earth magnetic field is not negligible with respect to the Coulomb scattering when the shower is young. Therefore the effect could increase for high altitude observations. In particular the shower extension along the East-West direction is larger than along the North-South direction (the opposite for the particle density). The different density of charged particles introduces an azimuthal modulation due to the different trigger efficiency of EAS detectors. This modulation was observed at the Yakutsk array for EAS with energy above $50\ PeV$ [2] and at the Alborz observatory for energy above $100\ TeV$ [3]. A North-South asymmetry has been observed also in EAS radio-experiments [4] and it can be explained as an effect of the geomagnetic Lorentz force on the EAS charged particles. Therefore the geomagnetic influence on the lateral distribution must be taken into account in the EAS simulation [5] and it was also suggested that a pointing correction is necessary for Čerenkov telescopes because of the geomagnetic field [6].

The effect of the geomagnetic field on the trigger efficiency of the ARGO-YBJ experiment was studied and simulated [7]. Due to the field B the average shift (d) of an electron (or positron) in the shower plane is

$$d = \frac{qh^2 B sin\chi}{2E_e cos^2\theta} \tag{1}$$

where χ is the angle between $\vec{B}$ and the particle velocity $\vec{v}$, q the electric charge, h the average vertical height of the electron path, E_e the average energy and θ the zenith angle. The trigger efficiency is connected to the size of the EAS footprint (lower particle density corresponds to lower trigger efficiency). Therefore the stretching of the EAS lateral distribution introduces a modulation with respect to the azimuth angle (ϕ). The azimuth distribution is expected to be

$$\frac{dN}{d\phi} = N_0 \left\{ 1 + g_1 cos\left(\phi + \phi_1\right) + g_2 cos\left[2\left(\phi + \phi_2\right)\right] \right\} \tag{2}$$

with $\phi_1 = \phi_2 = -\phi_B$ (ϕ_B is the azimuth of the geomagnetic field), $g_1 \propto sin2\theta$ and $g_2 \propto sin^2\theta$ if the modulation is totally geomagnetic. Furthermore [7]

$$\frac{g_1}{g_2} = \frac{sin2\theta_B}{sin^2\theta_B} \times \frac{sin2\theta}{sin^2\theta} \tag{3}$$

where θ_B is the zenith angle of the geomagnetic field.

1. ARGO-YBJ experiment

ARGO-YBJ is a full-coverage EAS experiment, located close to the YangBaJing village in Tibet (People's Republic of China) at $4300\ m$ above sea level. Its geographical coordinates are $90°31'50''E$ and $30°06'38''N$. The experiment is mainly devoted to Very High Energy (VHE) γ-astronomy and CR studies. The detector is essentially a continuous carpet ($78 \times 74\ m^2$) of Resistive Plate Counters. The detection area is enlarged to $110 \times 100\ m^2$ by means of a partially equipped guard ring. The time-space pattern allows a detailed reconstruction of showers induced by gamma and charged primaries.

In the ARGO-YBJ reference system the azimuth angle of EAS is defined with respect to the detector axes in the anticlockwise direction ($\phi = 0°$ for showers aligned with the x-axis and moving towards the positive direction). Thus the
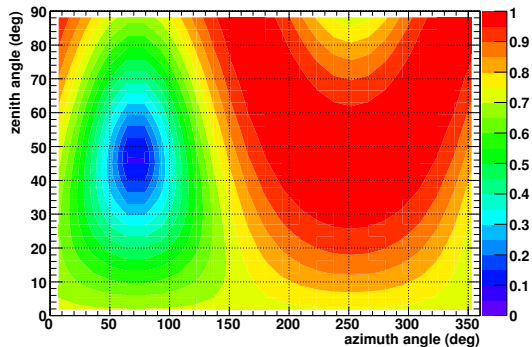
Figure 1. Absolute value of $sin\chi$ versus local angular coordinates (θ and ϕ) of the arrival direction of a charged particle in the ARGO-YBJ reference frame. χ is the angle between the magnetic field at YangBaJing and the velocity of the particle.

azimuth angle of showers going towards the geographical North is $\phi_N = 71.96° \pm 0.02°$. The quoted error is due to the measurement of the orientation of the detector axes with respect to the geographical reference system.

According to the International Geomagnetic Reference Field (IGRF) model available on the NOAA web site [8] at YangBaJing the geomagnetic field ($B = 49.7 \mu T$) has the following angular coordinates in the ARGO-YBJ reference system

$$\theta_B = 46.4°, \qquad \phi_B = 71.89°. \qquad (4)$$

The geomagnetic effect on primary CRs is negligible for the EAS collected by ARGO-YBJ. Thus we focus on the effects on the secondary particles in the shower. The Lorentz force acting on charged particles depends on the angle χ used in Eq. (1). The absolute value of $sin\chi$ is shown in Fig. 1 as a function of θ and ϕ. It has been checked that the variation with the height is negligible. In fact from $4.3 km$ up to $30 km$ above sea level the product $Bsin\chi$ changes less than 2%.

2. Data analysis

This analysis is based on the data collected in 3 days (October 12-14, 2010) with the trigger condition that at least 20 time-pixels (pads) are fired. In order to get a reliable reconstruction of the shower direction, the following cuts have been applied: shower core reconstructed inside a square of $40 \times 40 \ m^2$ at the center of the carpet, zenith angle lower than $60°$. After these cuts ~ 130 millions of events are selected.

The timing calibration of the pads has been performed according to the Characteristic Plane method [9]. This procedure removes the systematic time differences and arranges the time correction in order to make null the mean value of the

direction cosines. After this step a last premodulation correction is necessary in order to remove a small over-correction intrinsic to the method [10]. It is remarkable that small systematics in the timing calibration prevent the azimuthal analysis and the premodulation correction is crucial in order to get the proper ϕ-distribution.

The azimuthal distribution is shown in Fig. 2 together with a fit performed according to function (2). $\chi^2/ndf \sim 4$ and this is due to a small inefficiency at $\phi \sim n \times 90°$ ($n = 0, 1, 2, 3, 4$) which has not been examined here but does not invalidate this analysis. The fit results are

$$g_1 = (1.521 \pm 0.012)\%, \qquad \phi_1 = -72.43° \pm 0.47° \simeq -\phi_B,$$

$$g_2 = (0.587 \pm 0.012)\%, \qquad \phi_2 = -86.55° \pm 0.60° \neq -\phi_B.$$

The first coefficient is 3 times higher than the second one. The phase of the first harmonic results fully compatible with what expected. This is not the case for the phase of the second harmonic.

The geomagnetic origin of the modulation can be checked also by studying the dependence of the harmonic coefficients on the zenith angle. According to [7]

$$g_1 = k_1 \ sin2\theta, \qquad g_2 = k_2 \ sin^2\theta. \qquad (5)$$

This behaviour is verified for g_1 (see the fit in Fig. 3), not for g_2 (the plot is missing for room saving).

The unexpected result for the second harmonic cannot be explained as a consequence of some systematic error. The disagreement can be solved simply assuming a mix of geomagnetic and detector effects. The periodicity of a detector effect must be $180°$ and then acts only on the second harmonic, its phase must be $0°$ or $\pm 90°$ in connection with x and y-axes. The fit of Fig. 2 suggests the second solution because $\phi_2 = -86.55°$ is in-between $-\phi_B$ and $-90°$.

In this hypothesis the second harmonic can be splitted in two parts: one ($2B$) is due to the magnetic field, the other one ($2A$) can be originated
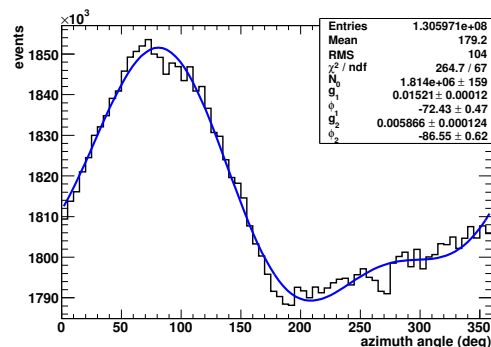

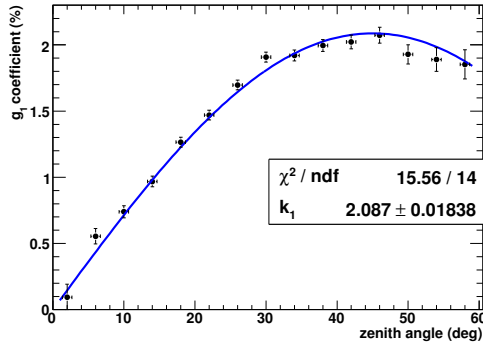Figure 2. Azimuthal distribution of EAS sample. Fit with function (2) is superimposed.

Figure 3. Coefficient g_1 versus the zenith angle. Function $g_1 = k_1\ sin2\theta$ is used for the superimposed fit.

k_1 (%)	2.101 ± 0.016
k_{2B} (%)	0.87 ± 0.32
ϕ_1 (°)	-71.86 ± 0.44
g_{2A}^{α} (%)	0.142 ± 0.024
g_{2A}^{β} (%)	0.350 ± 0.061
g_{2A}^{γ} (%)	1.25 ± 0.13
ϕ_{2A} (°)	-92.5 ± 2.9
χ^2/ndf	$491/209$

Table 1
Results of the fit with function (6) of the distributions in Fig. 4.

by a detector asymmetry. Three different data sets have been selected on the basis of the zenith value in order to disentagle these two effects. The ϕ-distributions of the 3 subsamples (α, β and γ in Fig. 4) can be fitted all together with a single function:

$$\frac{dN}{d\phi} = N_i \left\{ 1 + k_1 \langle sin2\theta \rangle_i\ cos\left(\phi + \phi_1\right) \right.$$
$$+ k_{2B} \langle sin^2\theta \rangle_i\ cos\left[2\left(\phi + \phi_1\right)\right]$$
$$\left. + g_{2A}^i\ cos\left[2\left(\phi + \phi_{2A}\right)\right] \right\} \qquad (6)$$

where the coefficients of the magnetic component are written using Eq.s (5), the magnetic phase is the same for first and second harmonic and the index $i = \alpha, \beta, \gamma$ indicates the subsamples. The quantities N_i, $\langle sin2\theta \rangle_i$ and $\langle sin^2\theta \rangle_i$ have been estimated separately for each subsample. Then the fit parameters are k_1, k_{2B}, ϕ_1, g_{2A}^{α}, g_{2A}^{β}, g_{2A}^{γ} and ϕ_{2A}. The result of this new fit is reported in Tab. 1. The value of k_1 is compatible with the fit in Fig. 3. The ratio $k_1/k_{2B} = 2.41 \pm 0.90$ is compatible with 1.9, value calculated according to (3) and (4). The magnetic phase is in perfect agreement with the expectation ($\phi_1 = -\phi_B$). It is remarkable that g_{2A}^i increases with θ and ϕ_{2A} is compatible with $-90°$ as expected for a detector effect.

A possible explanation of the detector origin of the harmonic $2A$ is that the pads have a different density along the detector axes ($1.54\ pads/m$ along x-axis and $1.76\ pads/m$ along y-axis). Taking into account the trigger requirement (at least 20 pads fired in a time-window of $420\ ns$) the different density can explain the higher trigger efficiency for showers along the y-axis ($\phi = \pm 90°$). The increasing of the effect with the zenith angle is the expected consequence of this hypothesis.

In order to check the results for the first harmonic we observe according to function (6) that the mean values of the direction cosines $\langle l \rangle$ and $\langle m \rangle$ of the showers depend on k_1 and ϕ_1 as in the following

$$\langle l \rangle = +\frac{k_1}{2}cos\phi_1 \langle sin2\theta\ sin\theta \rangle,$$

$$\langle m \rangle = -\frac{k_1}{2}sin\phi_1 \langle sin2\theta\ sin\theta \rangle.$$

In the analyzed sample the mean values are

$$\langle l \rangle = (12.12 \pm 0.29) \times 10^{-4}$$

$$\langle m \rangle = (35.56 \pm 0.30) \times 10^{-4}$$

$$\langle sin\ 2\theta\ sin\ \theta \rangle = (3588.39 \pm 0.20) \times 10^{-4}$$

As a consequence

$$k_1 = (2.094 \pm 0.016)\,\%, \qquad \phi_1 = -71.18° \pm 0.57°$$

These values are fully compatible with the the fit results in Tab. 1.

3. Simulation

Beams - In order to check the effect of the magnetic field on the data collection and on the EAS reconstruction, some "beams" of primary protons have been simulated with $\theta = 45°$, $E = 3\ TeV$ and interacting at $19\ km$ of height. The Corsika code [11] has been used to simulate the shower development and a GEANT-based code [12] to reproduce the detector response. Nine different beams have been generated with 3 different values of the azimuth angle ($\phi = 71.5°$ where $sin\chi \sim 0$, $\phi = 251.5°$ where $sin\chi$ is maximum and the intermediate angle $\phi = 161.5°$) and assuming 3 different values of the magnetic field (null, the effective magnetic field and twice the effective magnetic field). Negative and positive EAS components have been studied separately. It has been verified that the geomagnetic field separates positive and negative cores of about $4\ m$ right on the East-West direction. This stretching of the lateral distribution does not affect the combined reconstruction (positive + negative component) but acts on the trigger efficiency, according to [7]. The results are summarized in Tab. 2 and
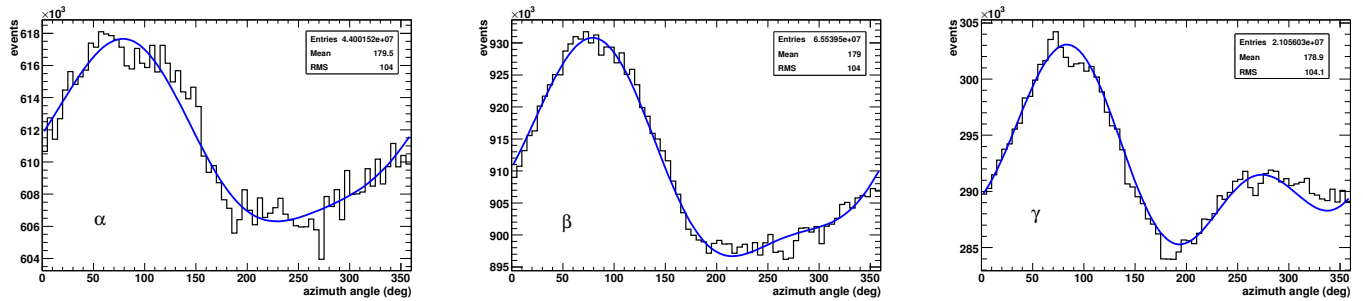
Figure 4. Azimuthal distribution in different θ-ranges ($0° - 20°$, $20° - 40°$ and $40° - 60°$). Fit with function (6) is superimposed.

ϕ	$sin\chi$	$B = 0\ \mu T$	$49.7\ \mu T$	$99.4\ \mu T$
$71.5°$	0.02	29.3%	29.4%	29.3%
$161.5°$	0.87	29.6%	28.4%	26.0%
$251.5°$	1.00	29.0%	27.7%	24.9%

Table 2
Trigger efficiency for simulated "beams" of CRs (see Sec. 3). Statistical error is 0.1%.

confirm that the trigger efficiency decreases as the geomagnetic field or the $sin\chi$ value increase.

Complete sample - A sample of proton and helium-induced EAS has been simulated in the energy range $10\ GeV - 10\ PeV$, with a uniform azimuthal distribution and the proper geomagnetic field. The analysis chain of the real data has been applied to the simulated ones, with the exception of the timing calibration that is not necessary for simulated data. The azimuthal distribution of triggered and selected events ($\sim 2 \times 10^6$) is not uniform (Fig. 5). The shape is similar to that of Fig. 2 and the parameters of the fit according to function (2) are almost compatible (the coefficients show larger discrepancies) but with large errors of the simulation fit. A larger simulation will be necessary in order to fix these few percent effects.

4. Conclusions

The modulation of the azimuthal distribution of a large EAS sample has been analyzed. The origin and the features of this modulation are fully understood. It is well described by means of two harmonics, the first one of the order of 1.5%, the second one of the order of 0.5%. The first harmonic is due to the geomagnetic Lorentz force on the shower charged particles. The second harmonic is the sum of magnetic and detector effects.

It is remarkable that in addition to the Moon shadow analysis the absolute pointing accuracy of EAS arrays could be tested also with deep studies concerning the azimuthal modulation.

REFERENCES

1. G. Cocconi, Phys. Review, 1954, **93**: 646-647. Erratum, Phys. Review, 1954, **95**: 1705-1706
2. A.A. Ivanov et al., JETP Letters, 1999, **69**: 288-293
3. M. Bahmanabadi et al., Experim. Astronomy, 2002, **13**: 39-57. M. Khakian Ghomi et al., Proceedings of 30th Intern. Cosmic Ray Conference, Merida, 2007
4. D. Ardouin et al. (CODALEMA Collaboration), Astropart. Physics, 2009, **31**: 192-200
5. A. Cillis, S.J. Sciutto, J. Phys. G: Nucl. Part. Physics, 2000, **26**: 309-321
6. S.C. Commichau et al., Nuclear Instrum. Methods A, 2008, **595**: 572-586
7. H.H. He et al., Proceedings of 29th Intern. Cosmic Ray Conference, Pune, 2005
8. www.ngdc.noaa.gov
9. H.H. He et al., Astropart. Physics, 2007, **27**: 528-532
10. G. Aielli et al. (ARGO-YBJ Collaboration), Astropart. Physics, 2009, **30**: 287-292
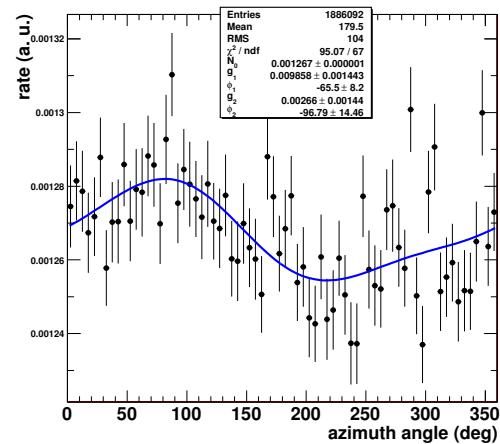11. www-ik.fzk.de/corsika/
12. wwwasd.web.cern.ch/wwwasd/geant/

Figure 5. Azimuthal distribution for simulated data and fit with function (2). The statistics does not allow to use function (6).